Received: 6 November 2020 | Revised: 4 February 2021 | Accepted: 5 February 2021

DOI: 10.1002/ardp.202000409

FULL PAPER

ARCH PHARM DPhG
Archiv der Pharmazie

Synthesis and docking calculations of tetrafluoronaphthalene derivatives and their inhibition profiles against some metabolic enzymes

Musa Erdoğan[1] | Parham Taslimi[2] | Burak Tuzun[3]

[1]Department of Food Engineering, Faculty of Engineering and Architecture, Kafkas University, Kars, Turkey

[2]Department of Biotechnology, Faculty of Science, Bartin University, Bartin, Turkey

[3]Chemistry Department, Science Faculty, Sivas Cumhuriyet University, Sivas, Turkey

Correspondence
Musa Erdoğan, Department of Food Engineering, Faculty of Engineering and Architecture, Kafkas University, 36100 Kars, Turkey.
Email: musaerdogan0@gmail.com

Parham Taslimi, Department of Biotechnology, Faculty of Science, Bartin University, 74100 Bartin, Turkey.
Email: ptaslimi@bartin.edu.tr and parham_taslimi_un@yahoo.com

Abstract

Syntheses of tetrahydroepoxy, *O*-allylic, *O*-prenylic, and *O*-propargylic tetrafluoronaphthalene derivatives, starting from 1-bromo-2,3,4,5,6-pentafluorobenzene, are reported here for the first time. The *O*-substituted tetrafluoronaphthalene derivatives were designed and also synthesized via a one-pot nucleophilic substitution reaction in excellent yields, whereas the tetrafluorotetrahydroepoxynaphthalene derivate was synthesized via a reduction reaction in excellent yield. The chemical structures of all the synthesized molecules were characterized by nuclear magnetic resonance, infrared spectroscopy, and high-resolution mass spectrometry techniques. In this study, a series of novel tetrafluoronaphthalene derivatives (**2**, **2a**, **4**–**6**) was tested toward several enzymes including α-glucosidase, acetylcholinesterase (AChE), and human carbonic anhydrase I and II (hCA I/II). The tetrafluoronaphthalene derivatives **2**, **2a**, and **4**–**6** showed IC_{50} and K_i values in the range of 0.83–1.27 and 0.71–1.09 nM against hCA I, 1.26–1.85 and 1.45–5.31 nM against hCA II, 39.02–56.01 and 20.53–56.76 nM against AChE, and 15.27–34.12 and 22.58–30.45 nM against α-glucosidase, respectively. Molecular docking calculations were made to determine the biological activity values of the tetrafluoronaphthalene derivatives against the enzymes. After the calculations, ADME/T analysis was performed to examine the effects on human metabolism. Finally, these compounds had antidiabetic and anticholinesterase potentials.

KEYWORDS
enzyme inhibition, molecular docking, *O*-allyl, *O*-prenyl, *O*-propargyl, tetrafluoronaphthalene

1 | INTRODUCTION

Fluorine atom is a small atom in size with very high electronegativity. Fluorine atoms bonded to carbon (C–F) have unique properties in organic chemistry.[1] The presence of a fluorine atom in a compound can efficiently affect pK_a, intrinsic potency, conformation, metabolic pathways, and pharmacokinetic and membrane permeability properties.[2] Organic compounds containing a fluorine atom influence the properties of a compound like absorption, distribution, excretion, and metabolism.[3] Fluorine is also often used to improve metabolic stability by blocking metabolically labile regions. Also, fluorine can balance biochemical properties like lipophilicity and basicity, and raise binding affinity to the target protein.[1,3] Fluoroaromatic skeletons are of interest in a variety of fields, such as physical and synthetic chemistry, environmental search, and biological tests (Figure 1).[4] Due to their unique biological and chemical properties, they are utilized in agrochemicals, bioactive components, optoelectronics, high-performance materials, and liquid crystalline materials.[5-10] They are also important building blocks for the synthesis of organofluorine-derived drugs (Figure 1).[11,12] In

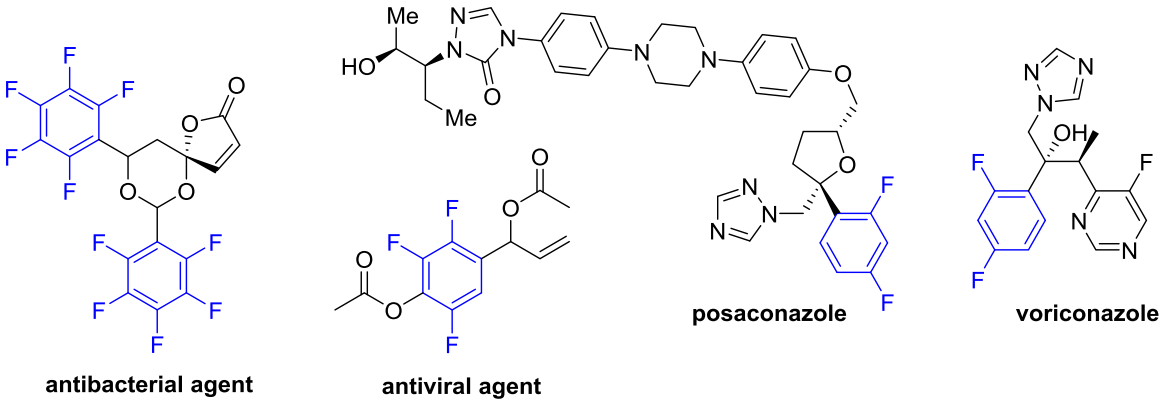

FIGURE 1 Bioactive molecules containing multifluoroaryl group

2003, according to data of the World Drug Index (WDI), 128 fluorinated pharmaceutical compounds having US trade names were reported.[1] For all these reasons, organic fluorine compounds have been receiving a great deal of attention from scientists in recent years.[13]

However, aromatic compounds containing the propargyl functional group are of considerable interest in the medicinal and analytical fields, and have long been recognized as mechanism-based inhibitors of CYPs.[14] They also function as a key pharmacophoric unit in acetylenic antibiotics, and these functional groups have been reported to contribute in enhancing lipophilicity.[15] In addition, prenylation and allylation are very interesting reactions, because they increase the lipophilic character and biological activity as compared with the unsubstituted derivates.[16,17]

CA helps maintain acid–base homeostasis, regulate pH, and fluid balance. CA Inhibitors are used to treat glaucoma, the excessive build up of water in the eyes. AZA given at 7–10 mg/kg three times daily causes self-limiting hyperchloremic metabolic acidosis, mild-to-moderate hypokalemia, and mild hypocalcemia in dogs.[18,19] Acetylcholinesterase (AChE) is an enzyme present in cholinergic neurons and its key role is the rapid breakdown of the neurotransmitter acetylcholine (ACh) released throughout neurotransmission. The level of the active site of AChE is a 20-Å length gorge that includes a catalytic anionic site and a peripheral anionic binding site.[20,21] In addition, AChE inhibitor compounds modulate ACh hydrolysis and also play an important role in diagnosing the cholinergic tone.[22,23] Type-2 diabetes mellitus (T2DM) is one of the most popular metabolic diseases in the world and is defined by hyperglycemia. α-Glucosidase enzymes are in the nutritive system that hydrolyzes carbohydrate molecules into glucose molecules.[24,25] One strategy that has been developed to treat T2DM is the inhibition of α-glucosidase enzyme using synthetic drugs.[26,27]

In recent studies, theoretical studies have become very common because theoretical calculations provide both time and financial gains.[28-30] Among the theoretical calculations made, the most used method is molecular docking. Biological activity values of molecules against enzyme proteins were calculated by the molecular docking program. The enzymes used for calculations are human carbonic anhydrase isoenzyme I (hCA I) (PDB ID: 3LXE),[31] human carbonic anhydrase isoenzyme II (hCA II) (PDB ID: 5AML),[32] AChE (PDB ID: 4M0E),[33] and α-glucosidase (PDB ID: 1R47).[34] After calculating the biological activities of the molecules, ADME/T (absorption, distribution, metabolism, excretion/toxicity) calculations were made for the use of the molecules as drugs.

However, tetrafluoronaphthalene derivatives containing *O*-propargyl, *O*-allyl, and *O*-prenyl groups are not common, and not much attention has been focused on these compounds in the literature. Therefore, we decided to synthesize new tetrafluoronaphthalene-based bioactive compounds that contain the important scaffolds for enzyme inhibition, namely tetrafluoronaphthalene and tetrahydroepoxy, *O*-allylic, *O*-prenylic, or *O*-propargylic units. With the above considerations in mind, as a part of biologically and pharmaceutically active units, here we reported on the synthesis and characterization of *O*-allylic, *O*-prenylic, and *O*-propargylic tetrafluoronaphthalene derivatives. In addition, it was aimed to investigate their effects on some important enzymes.

2 | RESULTS AND DISCUSSIONS

2.1 | Chemistry

Here, 5,6,7,8-tetrafluoronaphthalen-1-ol (**3**) was synthesized in two steps from 1-bromo-2,3,4,5,6-pentafluorobenzene (**1**) with the addition of furan via Diels–Alder cycloaddition reaction and acid-catalyzed aromatization reaction according to a previously reported method (Scheme 1).[35] Also, 5,6,7,8-tetrafluoro-1,2,3,4-tetrahydro-1,4-epoxynaphthalene was synthesized via reduction with hydrazine monohydrate of the compound **2** in EtOH in the presence of O_2 gas (Scheme 1).

The *O*-substituted tetrafluoronaphthalene derivatives **4**–**6** were synthesized via the nucleophilic substitution reaction of 5,6,7,8-tetrafluoronaphthalen-1-ol (**3**) with the propargyl, allyl-, and prenyl bromide in the presence of K_2CO_3 in dry acetone at reflux under a nitrogen atmosphere (Scheme 2).

SCHEME 1 Synthesis of the tetrafluoronaphthalene derivatives **2**, **2a**, and **3**

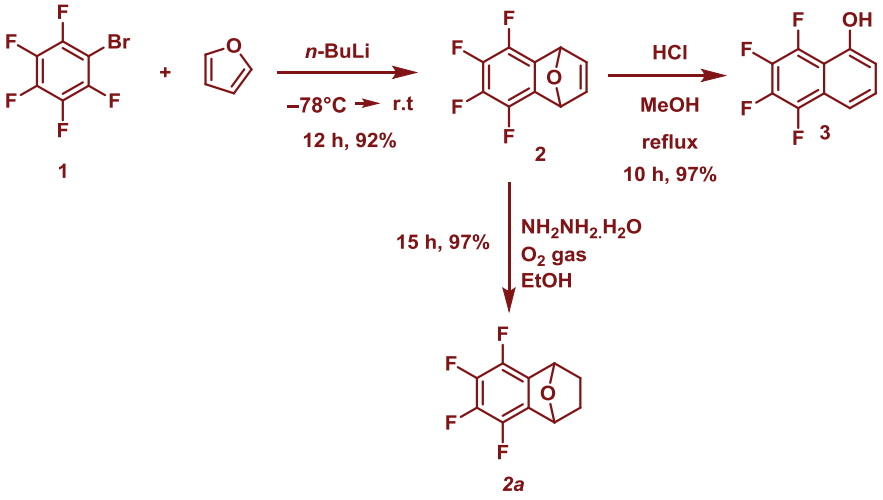

2.2 | Bioactivity results

The enzyme inhibitory effects of all the new tetrafluoronaphthalene derivatives (**2**, **2a**, **4**–**6**) were investigated against hCA I, hCA II as well as AChE, and α-glucosidase using the previous methods. The inhibitory activities were compared with standard compounds (Table 1 and Figure 2). The following results were recorded.

CA inhibitor compounds (CAIs) can be grouped into two major classes: some inhibitor compounds that bind to the active site coordinating the catalytic zinc ion, like primary sulfonamide compounds and their isosteres (sulfamides and sulfamates), xanthates, and dithiocarbamates, and inhibitor compounds that bind to the active site without interacting with the metal ion.[36,37] Compounds belonging to this second group can either be anchored to the zinc-bound water molecule, as reported for polyamines and phenols, or bind in different regions of the active site observed for lacosamide and coumarin.[38,39] Indeed, some inhibitor compounds like carboxylic acids can show both the binding modes, depending on their chemical structure.[40] The target novel tetrafluoronaphthalene derivatives (**2**, **2a**, **4**–**6**) were screened for their potentials against the two cytosolic hCA isoforms, namely hCA I and hCA II, using acetazolamide (AZA) as a standard. The inhibition modes and K_i constants of the new tetrafluoronaphthalene derivatives (**2**, **2a**, **4**–**6**) were calculated from Lineweaver–Burk[41] graphs, as explained previously.[42,43] The new tetrafluoronaphthalene derivatives (**2**, **2a**, **4**–**6**) showed nanomolar ranges against hCA I with K_i values between 0.71 ± 0.15 and 1.09 ± 0.17 nM (Table 1). Indeed, compound **6** had the best

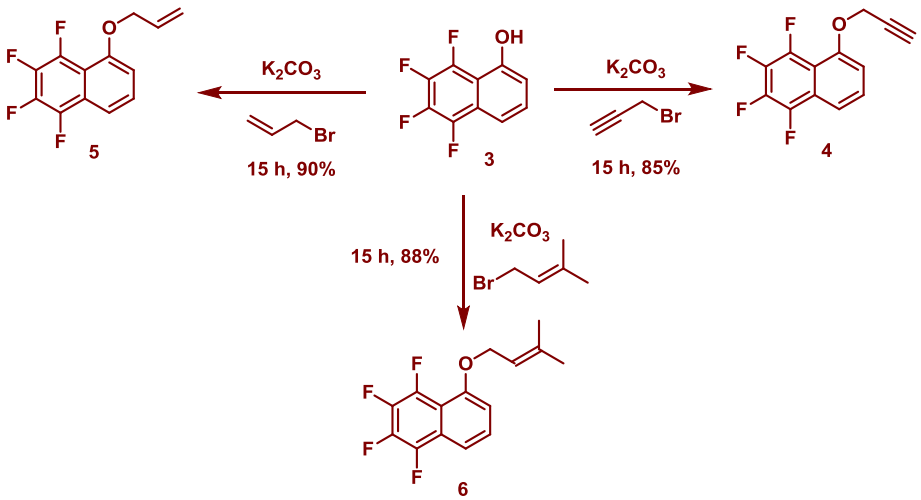

SCHEME 2 Synthesis of *O*-allylic, *O*-prenylic, and *O*-propargylic tetrafluoronaphthalene derivatives **4**–**6**

TABLE 1 The enzyme inhibition results of novel tetrafluoronaphthalene derivatives (**2**, **2a**, **4**–**6**) against human carbonic anhydrase isoenzymes I and II (hCA I and II), acetylcholinesterase (AChE), and α-Gly enzymes

Compounds	IC_{50} (nM)								K_i values (nM)			
	hCA I	r^2	hCA II	r^2	AChE	r^2	α-Gly	r^2	hCA I	hCA II	AChE	α-Gly
2	1.27	0.9627	1.85	0.9923	39.02	0.9528	24.95	0.9626	1.02 ± 0.22	4.37 ± 0.80	20.53 ± 3.82	24.35 ± 2.74
2a	1.02	0.9916	1.76	0.9986	56.01	0.9824	15.27	0.9892	1.09 ± 0.17	3.37 ± 0.70	22.72 ± 6.52	22.58 ± 6.28
4	0.95	0.9889	1.52	0.9690	50.23	0.9518	30.41	0.9472	0.88 ± 0.07	5.31 ± 1.52	22.86 ± 4.73	26.51 ± 6.76
5	0.83	0.9627	1.26	0.9962	45.71	0.9025	34.12	0.9673	0.82 ± 0.24	1.45 ± 0.14	36.77 ± 4.87	30.45 ± 7.73
6	0.98	0.9782	1.38	0.9827	42.16	0.9488	31.88	0.9902	0.71 ± 0.15	2.01 ± 0.55	56.76 ± 11.12	29.88 ± 5.76
AZA[a]	1.48	0.9622	2.32	0.9340	–	–	–	–	2.47 ± 0.80	4.02 ± 0.92	–	–
TAC[a]	–	–	–	–	98.28	0.9817	–	–	–	–	56.72 ± 13.76	–
ACR[a]	–	–	–	–	–	–	48.13	0.9690	–	–	–	51.48 ± 3.93

Abbreviations: AChE, acetylcholinesterase; ACR, acarbose; AZA, acetazolamide; hCA I, human carbonic anhydrase isoenzyme I; hCA II, human carbonic anhydrase isoenzyme II; TAC, tacrine; α-Gly, α-glucosidase.

[a]Standard compounds.

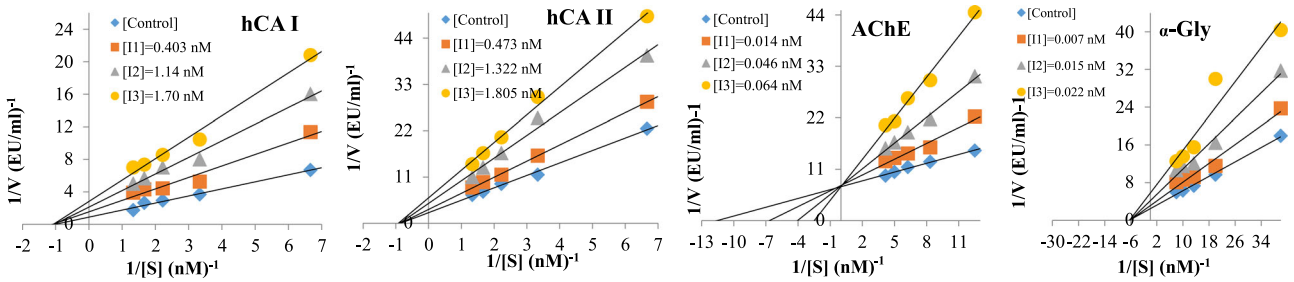

FIGURE 2 Determination of Lineweaver–Burk graphs for excellent inhibitors of human carbonic anhydrase isoenzymes I and II (hCA I and II), acetylcholinesterase (AChE), and α-glucosidase (α-Gly)

inhibition effect (K_i: 0.71 ± 0.15 nM). AZA exhibited a K_i value of 2.47 ± 0.80 nM for cytosolic hCA I isoenzyme ($K_{i\text{-AZA}}/K_{i\text{-}6}$: 3.47). The results clearly displayed that the novel tetrafluoronaphthalene derivatives (**2**, **2a**, **4**–**6**) had an effective inhibition profile than that of AZA against hCA I isoform (Table 1 and Figure 2). Regarding the inhibition effects against hCA II, the tested novel tetrafluoronaphthalene derivatives (**2**, **2a**, **4**–**6**) demonstrated a similar inhibition potency with K_i values ranging from 1.45 ± 0.14 to 5.31 ± 1.52 nM. However, AZA as control had a K_i value of 4.02 ± 0.92 nM against hCA II. As can be seen in Table 1, compound **5** had the greatest selectivity against hCA II isoenzyme. Indeed, it had a maximum inhibition profile and can be used for the treatment of glaucoma after advanced examinations ($K_{i\text{-AZA}}/K_{i\text{-}5}$: 2.77) (Table 1). Furthermore, recently, CA inhibitors were shown to be of potential use in the management of cerebral ischemia, neuropathic pain, and arthritis, which are conditions for which this class of pharmacologic agents was previously considered inappropriate.[44] However, the attentive search for novel classes of compounds with efficacy and selectivity for the different isoforms involved in these quite diverse conditions resulted in proof-of-concept studies, which have suggested that all catalytically active hCA isoforms may be considered as interesting drug targets.[45,46]

Cholinergic neurotransmission plays a key role in impaired cognitive function in Alzheimer's disease (AD) and adult-onset dementia disorders. Treatments to counteract amyloid accumulation, tau hyperphosphorylation, and immunotherapy have been recommended, but they failed to produce effects and were therefore discontinued in Phase II or III clinical trials.[47,48] At present, enhancement of cholinergic neurotransmission still represents the main approach to symptomatic treatment of cognitive and behavioral symptoms of mild and moderate stages of AD. In line with this therapeutic strategy, various molecules like linopirdine, an agent that increases hippocampus ACh release, muscarinic ACh receptor agonists like xanomeline, and AChE inhibitor compounds like tacrine and physostigmine were used.[49,50] These cholinergic enzyme inhibition results are reported in Table 1. The novel tetrafluoronaphthalene derivatives (**2**, **2a**, **4**–**6**) had K_i values ranging from 20.53 ± 3.82 to 56.76 ± 11.12 nM for AChE (Table 1), whereas TAC had a K_i value of 56.72 ± 13.76 nM against the indicated AChE enzyme. It could be seen from the table that all novel molecules demonstrated marked

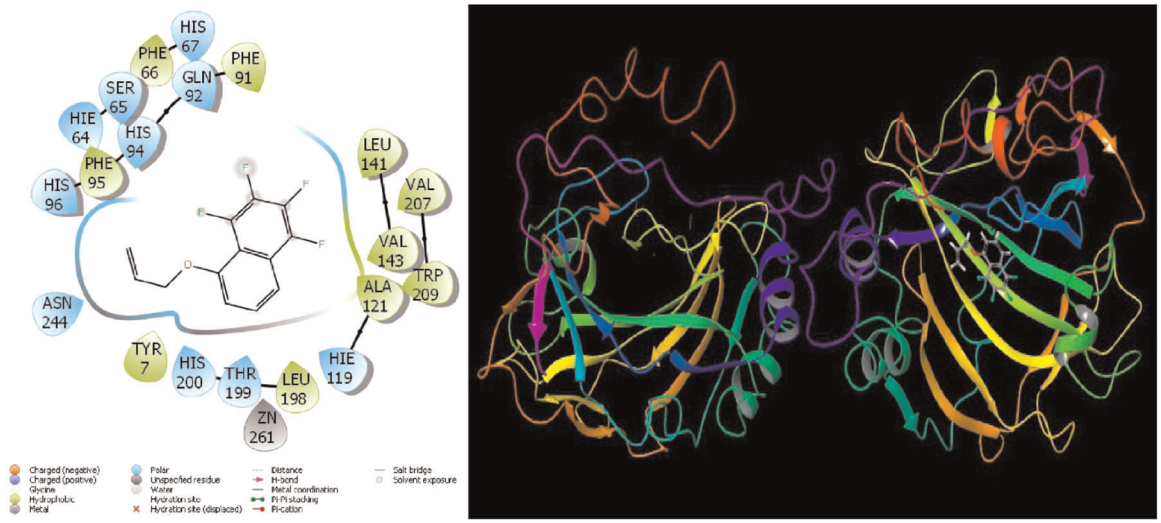

FIGURE 3 Presentation of interactions of the compound **5** with human carbonic anhydrase isoenzyme I enzyme

inhibitory effects against both cholinesterase with K_i values ranging in sub-nanomolar ranges; however, compound **2** showed a perfect inhibition effect against AChE (K_i: 20.53 ± 3.82 nM; $K_{i\text{-}TAC}/K_{i\text{-}2}$: 2.88) (Table 1).

Finally, for the α-glucosidase, the novel tetrafluoronaphthalene derivatives (**2**, **2a**, **4**–**6**) showed K_i values between 22.58 ± 6.28 and 30.45 ± 7.73 nM (Table 1). The results demonstrated that compound **2** had effective α-glucosidase inhibition effects than that of acarbose (ACR, K_i: 51.48 ± 3.93 nM) as a standard α-glucosidase inhibitor. Also, highly effective K_i values were calculated for compound **2a** (K_i: 22.58 ± 6.28 nM). Inhibitors of this enzyme delay the breakdown of carbohydrate molecules in the small intestine and diminish the postprandial blood glucose excursion; hence, inhibition of glucosidase enzyme has an important effect on polysaccharide metabolism, cellular interaction, and glycoprotein processing, widening opportunities for the discovery of new therapeutic factors against diseases like obesity, viral infection, diabetes, and metastatic cancer.[51]

Indeed, AG as a glucosidase located in the brush border of the small intestine is able to selectively hydrolyze terminal (1 → 4)-linked α-glucose residues (disaccharides or starch) to release a single α-glucose molecule.[52]

2.3 | Molecular docking

Molecular docking calculations were made to compare the biological activities of molecules. With these calculations, many

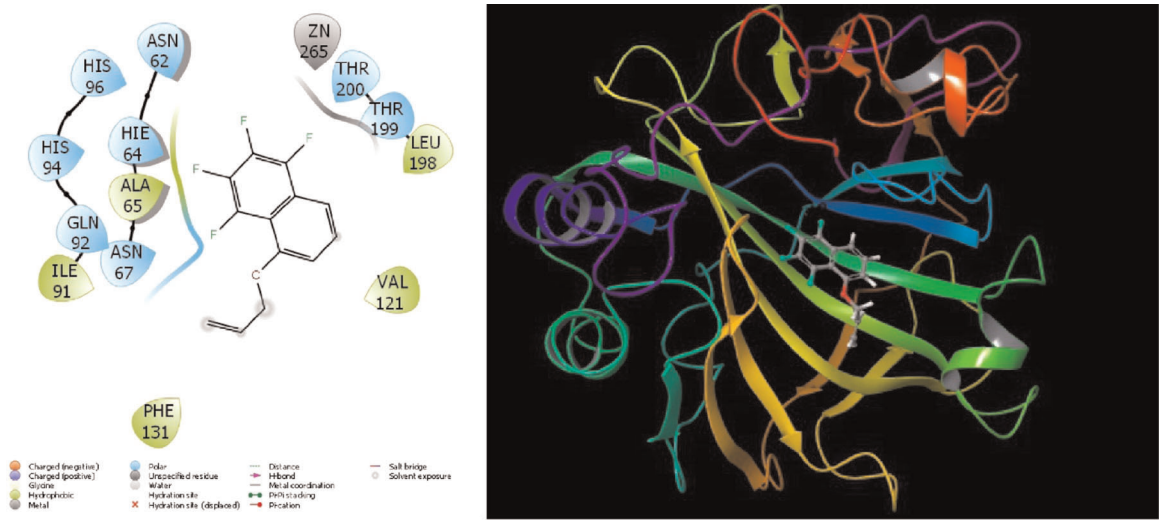

FIGURE 4 Presentation of interactions of the compound **5** with human carbonic anhydrase isoenzyme II enzyme

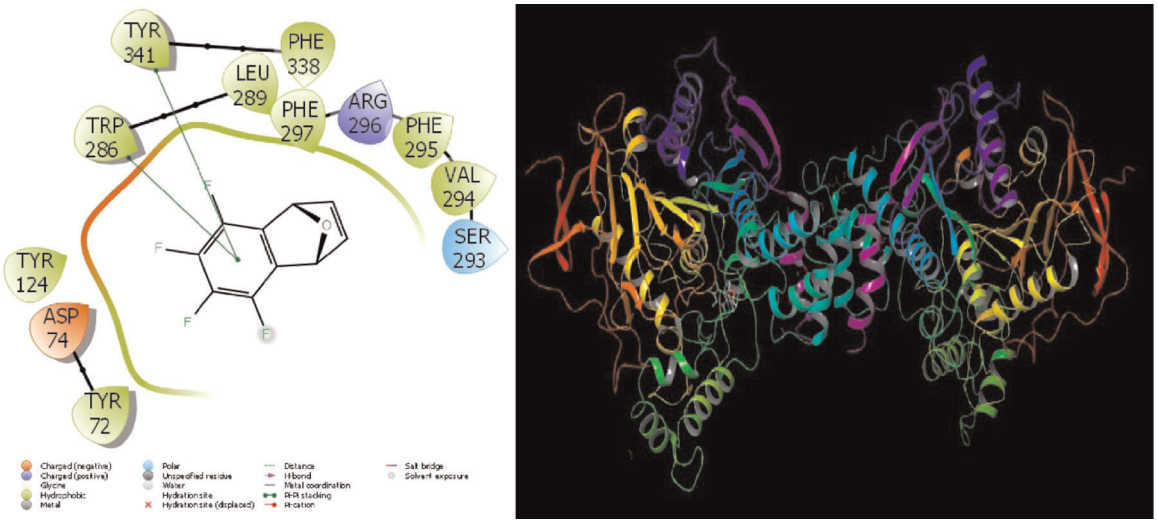

FIGURE 5 Presentation of interactions of the compound **2** with acetylcholinesterase enzyme

parameters were obtained to compare enzymes against protein biological activities. Each obtained parameter gave information about the different chemical properties of the molecules. The parameter used to compare biological activity between these parameters is the docking score. If the numerical value of this parameter of a molecule is more negative than other molecules, the biological activity of this molecule is higher than others.[53] The most important factor affecting the numerical value of this parameter is chemical interactions between molecules and proteins. As the chemical interactions between molecules and proteins increase, the biological activities of the molecules increase.[54] These interactions include hydrogen bonds, polar and hydrophobic interactions, π–π interactions, and halogen interactions.[55-61] The interaction of enzymes with the molecule with the highest biological activity is shown in Figures 3-6.

Other parameters obtained from the interactions of molecules against enzymes are given in Table 2. Among other parameters, Glide ligand efficiency, Glide ecoul, and Glide emodel are the parameters obtained as a result of chemical interactions of molecules.[62] However, other parameters obtained are Glide energy, Glide einternal, and Glide posenum parameters that occur from the pose formed between enzymes and molecules.[63]

After comparing the biological activity of tetrafluoronaphthalene derivatives against protein of enzymes, ADME/T analysis was conducted to theoretically predict the effects and responses of tetrafluoronaphthalene derivatives on human metabolism. As a result of this theoretical analysis, many parameters have been obtained and these parameters are given in Table 3. The first parameter among these parameters is the solute molecular weight, which requires the molecule to have a specific molecular weight. Another parameter is

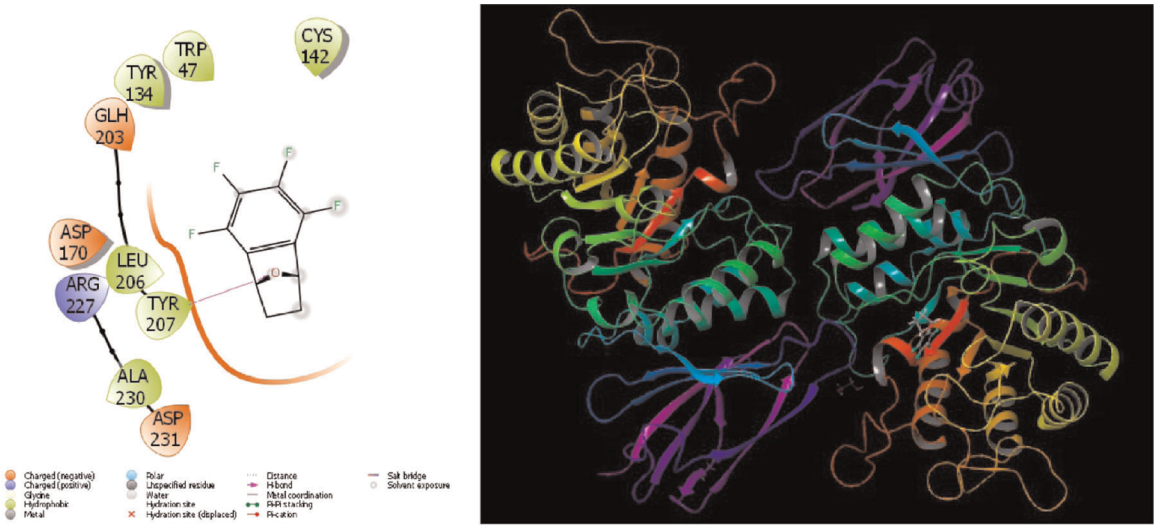

FIGURE 6 Presentation of interactions of the compound **2a** with α-glucosidase enzyme

TABLE 2 Numerical values of the docking parameters of molecule against enzymes

hCA I	Docking score	Glide ligand efficiency	Glide hbond	Glide evdw	Glide ecoul	Glide emodel	Glide energy	Glide einternal	Glide posenum
2	−4.95	−0.33	−0.32	−21.21	−4.01	−33.43	−25.22	0.00	290
2a	−4.95	−0.33	−0.32	−21.29	−4.12	−33.70	−25.41	0.00	374
4	−4.10	−0.23	0.00	−29.15	−0.23	−37.57	−29.38	0.32	293
5	−5.83	−0.21	0.00	−26.81	−1.46	−34.87	−28.26	0.95	290
6	−4.56	−0.23	0.00	−28.22	−2.95	−39.14	−31.16	2.33	36

hCA II	Docking score	Glide ligand efficiency	Glide hbond	Glide evdw	Glide ecoul	Glide emodel	Glide energy	Glide einternal	Glide posenum
2	−4.58	−0.31	0.00	−18.61	−4.17	−30.08	−22.79	0.00	117
2a	−5.40	−0.36	−0.32	−17.23	−4.37	−29.85	−21.60	0.00	325
4	−3.29	−0.18	0.00	−27.58	−0.77	−34.35	−28.34	0.16	366
5	−5.70	−0.21	0.00	−22.25	−3.11	−30.71	−25.36	1.14	131
6	−4.43	−0.22	0.00	−29.61	−0.64	−34.31	−30.25	6.98	105

AChE	Docking score	Glide ligand efficiency	Glide hbond	Glide evdw	Glide ecoul	Glide emodel	Glide energy	Glide einternal	Glide posenum
2	−6.36	−0.41	0.00	−23.33	−0.35	−32.26	−23.68	0.00	53
2a	−6.21	−0.41	0.00	−20.57	−1.73	−30.66	−22.31	0.00	355
4	−5.80	−0.32	0.00	−26.24	−3.61	−40.57	−29.85	0.46	383
5	−6.16	−0.34	0.00	−25.00	−3.06	−38.65	−28.06	1.20	269
6	−6.35	−0.32	−0.03	−22.72	−5.13	−38.92	−27.85	0.95	86

α-Gly	Docking score	Glide ligand efficiency	Glide hbond	Glide evdw	Glide ecoul	Glide emodel	Glide energy	Glide einternal	Glide posenum
2	−3.99	−0.27	−0.17	−15.99	−2.46	−22.95	−18.45	0.00	262
2a	−4.03	−0.27	−0.18	−15.93	−2.91	−23.53	−18.84	0.00	319
4	−3.52	−0.20	0.00	−21.41	−2.13	−29.06	−23.54	0.26	300
5	−3.28	−0.18	0.00	−22.14	−0.65	−27.73	−22.79	0.22	74
6	−3.81	−0.19	0.00	−22.84	−1.92	−30.39	−24.77	1.18	27

Abbreviations: AChE, acetylcholinesterase; ACR, acarbose; AZA, acetazolamide; hCA I, human carbonic anhydrase isoenzyme I; hCA II, human carbonic anhydrase isoenzyme II; TAC, tacrine; α-Gly, α-glucosidase.

PISA, also known as solute total SASA. This parameter is the π (carbon and attached hydrogen) component of the SASA. Another parameter is QP polarizability, which is the predicted polarizability in cubic angstroms. Another important parameter is the QPlogHERG, which is the numerical value of the estimated IC_{50} value when HERG K channels are blocked. The next parameter is QPPCaco, which is the Caco-2 cell permeability at the gut–blood barrier for inactive transport. Another parameter is the QPlogBB, which is the coefficient of the brain–blood barrier of an orally administered drug. The next parameter is human oral absorption, which is the predicted qualitative human oral absorption: 1, 2, or 3 for low, medium, or high.[64-66]

Among all ADME/T parameters, the two most important parameters are the Rule of Five and the Rule of Three. The Rule of Five[67,68] and Rule of Three[69] parameters are more important than any other parameter. The numerical value of these two parameters is expected to be zero. The Rule of Five parameter, also known as Lipinski's rule of five, is Pfizer's fifth rule. The rules are as follows: mol MW < 500, QPlog *P* o/w < 5, donorHB ≤ 5, accptHB ≤ 10. However, the rule of three parameter is known as Jorgensen's rule of three. The three rules are as follows: QPlog *S* > −5.7, QPPCaco > 22 nm/s, #primary metabolites < 7. If the numerical value of the rule of three parameter is zero, this molecule can be used orally as a drug. The last and another important parameter is Jm, which is the predicted

TABLE 3 ADME properties of the compounds

	2	2a	4	5	6	Reference range
mol_MW	216	218	254	256	284	130 to 725
Dipole (D)	3.5	3.6	6.2	6.0	6.7	1.0 to 12.5
SASA	353	360	454	454	522	300 to 1000
FOSA	53	155	82	102	198	0 to 750
FISA	0	0	0	0	0	7 to 330
PISA	137	44	225	213	179	0 to 450
WPSA	162	161	148	139	145	0 to 175
Volume ($Å^3$)	570	588	739	752	875	500 to 2000
donorHB	0	0	0.5	0	0	0 to 6
accptHB	2	2	1	1	1	2.0 to 20.0
glob (sphere = 1)	0.9	0.9	0.9	0.9	0.8	0.75 to 0.95
QPpolrz ($Å^3$)	18.0	17.8	23.6	24.1	28.6	13.0 to 70.0
QPlogPC16	3.8	3.3	5.7	5.8	6.6	4.0 to 18.0
QPlogPoct	7.0	6.8	9.4	8.8	10.3	8.0 to 35.0
QPlogPw	3.2	2.6	3.2	2.4	2.3	4.0 to 45.0
QPlogPo/w	3.4	3.2	5.1	5.0	5.7	−2.0 to 6.5
QPlogS	−2.3	−2.5	−4.9	−5.0	−6.3	−6.5 to 0.5
CIQPlogS	−2.3	−2.5	−4.9	−5.0	−6.3	−6.5 to 0.5
QPlogHERG	−3.1	−2.7	−4.7	−4.5	−4.8	[a]
QPPCaco (nm/s)	9906	9906	9906	9906	9906	[b]
QPlogBB	−0.5	−0.3	0.0	0.1	0.2	−3.0 to 1.2
QPPMDCK (nm/s)	10,000	10,000	10,000	10,000	10,000	[b]
QPlogKp (Kp in cm/h)	−1.0	−1.4	−0.4	−0.5	−0.6	
IP (eV)	10.5	10.5	9.0	9.0	9.0	7.9-10.5
EA (eV)	1.1	1.1	1.5	1.5	1.4	−0.9 to 1.7
#metab	3	3	2	2	4	1 to 8
QPlogKhsa	−0.2	−0.1	0.4	0.5	0.8	−1.5 to 1.5
Human oral absor.	3	3	3	3	1	-
Per. human oral absor.	100	100	100	100	100	[c]
PSA	10.1	9.9	6.0	4.6	5.6	7 to 200
Rule of Five	0	0	1	1	1	Maximum is 4
Rule of Three	0	0	0	0	1	Maximum is 3
Jm	101.5	31.4	1.3	0.8	0.0	-

[a]Concern below −5.

[b]$a < 25$ is poor and $a > 500$ is great.

[c]$b < 25$ is poor and $b > 80$ is high.

maximum transdermal transport rate, $K_p \times MW \times S$ (μg/cm^2/h). K_p and S are obtained from the aqueous solubility and skin permeability, QPlog Kp and QPlog S. These parameters are the numerical values of a theoretical parameter calculated for the application of molecules that can be drugs to the skin.

3 | CONCLUSION

In conclusion, we designed, synthesized, and characterized biologically important novel tetrafluoronaphthalene derivatives that contain the important scaffolds for enzyme inhibition, namely

tetrahydroepoxy, *O*-allylic, *O*-prenylic, and *O*-propargylic units, and tetrafluoronaphthalene skeleton. However, these novel tetrafluoronaphthalene derivatives (**2**, **2a**, **4**–**6**) were recorded to have anticholinesterase and antidiabetic properties; also, they are appropriate for future significant drug searches. These new compounds had antidiabetic and anticholinesterase potentials. Biological activities of tetrafluoronaphthalene derivatives against enzymes were compared. Afterward, a theoretical ADME/T analysis of these molecules was performed. As a result of these analyses, it was examined with many parameters. When the numerical values of the obtained parameters are examined, it is perceived that they may be studied as active and effective new drugs in future in vivo and in vitro studies.

4 | EXPERIMENTAL

4.1 | Chemistry

4.1.1 | General

All reactions were carried out under nitrogen and monitored by thin-layer chromatography (TLC) method, and spots were visualized by UV irradiation. All solvents were dried and distilled before use. Melting points are uncorrected. IR spectra were recorded on a PerkinElmer FTIR spectrometer. The one- and two-dimensional ^{1}H and ^{13}C nuclear magnetic resonance (NMR) spectra (see the Supporting Information) were recorded on a Bruker-400 spectrometer using tetramethylsilane as the internal standard. All spectra were recorded at 25°C, and coupling constants (*J* values) are given in hertz (Hz). Chemical shifts are given in parts per million (ppm). Mass spectra were recorded on a 6530 Accurate-Mass Q-TOF-LC/MS from Agilent Technologies. TLC was performed on silica gel 60 HF254 aluminum plates (Fluka).

The InChI codes of the investigated compounds, together with some biological activity data, are provided as Supporting Information.

4.1.2 | Synthetic procedure for the preparation of compounds **2, 2a, 3–6**

*5,6,7,8-Tetrafluoro-1,4-dihydro-1,4-epoxynaphthalene (**2**)*

5,6,7,8-Tetrafluoro-1,4-dihydro-1,4-epoxynaphthalene (**2**) was synthesized according to a previously reported method in the literature.[35] Yield 92%, white crystals, M.p. 61–63°C, (lit.[35] sublimed 80–90°C), ^{1}H NMR (400 MHz, $CDCl_3$): δ = 7.08 (s, 2H), 6.02 (s, 2H). ^{13}C NMR (100 MHz, $CDCl_3$): δ = 142.69 (s), 142.32 (dt, *J* = 10.5, 4.2 Hz), 140.12–139.64 (m), 138–136.76 (m), 130.39 (dd, *J* = 14.5, 8.4 Hz), 80.09 (s). ^{19}F NMR (376 MHz, $CDCl_3$): δ = −143.04 (m), −157.20 (m).

*5,6,7,8-Tetrafluoro-1,2,3,4-tetrahydro-1,4-epoxynaphthalene (**2a**)*

In a round-bottom flask, 5,6,7,8-tetrafluoro-1,4-dihydro-1,4-epoxynaphthalene (**2**) (0.30 g, 1.39 mmol) and EtOH (30 ml) were added. To this mixture, NH_2–NH_2·H_2O (0.277, 5.55 mmol) was added, and the reaction was completed under an atmosphere of O_2 gas. The mixture was stirred at 40°C for 15 h and monitored by TLC. On completion of the reaction, the solvent was removed with a rotary evaporator and the crude product was extracted with EtOAc, and the organic phases were dried (Na_2SO_4), filtered, and evaporated. After evaporation of the solvent and purification by column chromatography on silica gel by eluting with *n*-hexane/EtOAc of increasing polarity, 5,6,7,8-tetrafluoro-1,2,3,4-tetrahydro-1,4-epoxynaphthalene (**2a**) (0.295 g, yield 97% in *n*-hexane/EtOAc 85:15) was obtained as a brown solid. M.p. 63–65°C, ^{1}H NMR (400 MHz, $CDCl_3$): δ = 5.67 (d, *J* = 1.2 Hz, 2H), 1.13–2.10 (m, AA′ of AA′BB′, 2H), 1.48–1.42 (m, BB′ of AA′BB′, 2H). HRMS (Q-TOF): *m/z* [M ($C_{10}H_6F_4O$)–$C_1F_4O_1$]$^{+}$ calcd. for C_9H_{11}: 119.0860; found: 119.0771.

*5,6,7,8-Tetrafluoronaphthalen-1-ol (**3**)*

5,6,7,8-Tetrafluoronaphthalen-1-ol (**3**) was synthesized according to a previously reported method in the literature.[21] Yield 97%, white solid: M.p. 126°C (lit.[16] M.p. 126–127°C). ^{1}H NMR (400 MHz, $CDCl_3$): δ = 7.64 (d, *J* = 8.5, 1H), 7.47 (t, *J* = 8.1, 1H), 7.05 (d, *J* = 7.7, 1H), 6.5 (s, 1H, –OH).

*1,2,3,4-Tetrafluoro-5-(prop-2-yn-1-yloxy)naphthalene (**4**)*

To 5,6,7,8-tetrafluoronaphthalen-1-ol (**3**) (0.500 g, 2.52 mmol) in acetone (40 ml), K_2CO_3 (0.697 g, 5.05 mmol) and propargylbromide (0.230 ml, 3.03 mmol) were added. The mixture was refluxed for 15 h at 60°C under an N_2 atm. Then, the solvent was evaporated with a rotary evaporator and the crude product was diluted in cold water (50 ml). The aqueous mixture was extracted with EtOAc (3 × 30 ml), and the organic layers were dried (Na_2SO_4), filtered, and evaporated. The crude product was purified via 1,2,3,4-tetrafluoro-5-(prop-2-yn-1-yloxy)naphthalene (**4**) (546 mg, 85%). White solid: mp 70–72°C. IR (cm^{-1}) ν_{max} 3311, 2931, 2875, 2139, 1942, 1835, 1727, 1663, 1601, 1523, 1485, 1411, 1388, 1273, 1238, 1130, 1090, 1026, 976, 964, 888, 841, 792, 764, 746, 701. ^{1}H NMR (400 MHz, $CDCl_3$): δ = 7.65 (d, *J* = 8.5 Hz, 1H), 7.50 (t, *J* = 8.1 Hz, 1H), 7.09 (d, *J* = 7.7 Hz, 1H), 4.87 (d, *J* = 2.2 Hz, 2H), 2.56 (t, *J* = 2.2 Hz, 1H). HRMS (Q-TOF): *m/z* [M]$^{+}$ calcd. for $C_{13}H_6F_4O$: 254.03548; found: 254.03434.

*5-(Allyloxy)-1,2,3,4-tetrafluoronaphthalene (**5**)*

To 5,6,7,8-tetrafluoronaphthalen-1-ol (**3**) (0.50 g, 2.52 mmol) in acetone (40 ml), K_2CO_3 (0.697 g, 5.05 mmol) and allylbromide (0.262 ml, 3.03 mmol) were added. The reaction mixture was refluxed for 15 h at 60°C under an N_2 atm. Then, the solvent was evaporated with a rotary evaporator and the crude product was diluted in cold water (50 ml). The mixture was extracted with EtOAc (3 × 30 ml), and the organic layers were dried (Na_2SO_4), filtered, and evaporated. The crude product was purified via column chromatography on silica gel (75 g) by eluting with 25% EtOAc/*n*-hexane to give 5-(allyloxy)-1,2,3,4-tetrafluoronaphthalene (**5**) (583 mg, 90%). White solid: mp 50–52°C. IR (cm^{-1}) ν_{max} 3096, 2994, 2917, 2868, 1935, 1836, 1665, 1605, 1523, 1487, 1472, 1411, 1367, 1271, 1247, 1128, 1094, 1021, 971, 935, 886, 843, 792, 746, 701. ^{1}H NMR (400 MHz, $CDCl_3$): δ = 7.62 (d, *J* = 8.4 Hz, 1H), 7.45 (t, *J* = 8.1 Hz, 1H), 6.89 (d, *J* = 7.7 Hz, 1H), 6.19–6.08 (m, 1H), 5.59 (d,

J = 17.3 Hz, 1H), 5.37 (d, J = 10.6 Hz, 1H), 4.69 (d, J = 1.5 Hz, 2H). HRMS (Q-TOF): m/z $[M]^+$ calcd. for $C_{13}H_8F_4O$: 256.05113, 257.05448; found: 256.04960, 257.0533.

*1,2,3,4-Tetrafluoro-5-[(3-methylbut-2-en-1-yl)oxy]naphthalene (**6**)*

To 5,6,7,8-tetrafluoronaphthalen-1-ol (**3**) (0.50 g, 2.52 mmol) in acetone (40 ml), K_2CO_3 (0.697 g, 5.05 mmol) and prenyl bromide (0.350 ml, 3.03 mmol) were added. The reaction mixture was refluxed for 15 h at 60°C under an N_2 atm. Then, the solvent was evaporated with a rotary evaporator and the crude product was diluted in cold water (50 ml). The mixture was extracted with EtOAc (3 × 30 ml), and the organic layers were dried (Na_2SO_4), filtered, and evaporated. The crude product was purified via column chromatography on silica gel (75 g) by eluting with 25% EtOAc/*n*-hexane to give 1,2,3,4-tetrafluoro-5-[(3-methylbut-2-en-1-yl)oxy]naphthalene (**6**) (635 mg, 88%). White solid: mp 52–54°C. IR (cm^{-1}) ν_{max} 2991, 2966, 2938, 2916, 2871, 1931, 1833, 1661, 1608, 1526, 1488, 1471, 1413, 1365, 1323, 1274, 1237, 1199, 1178, 1133, 1094, 1024, 965, 888, 785, 764, 746, 699. ^{1}H NMR (400 MHz, $CDCl_3$): δ = 7.55 (d, J = 8.4 Hz, 1H), 7.45 (t, J = 8.1 Hz, 1H), 6.92 (d, J = 7.7 Hz, 1H), 5.58 (t, J = 6.3 Hz, 1H), 4.68 (d, J = 6.3 Hz, 2H), 1.84 (s, 3H), 1.79 (s, 3H). HRMS (Q-TOF): m/z $[M-H]^+$ calcd. for $C_{15}H_{11}F_4O$: 283.07460, 284.07796; found: 283.07121, 284.07934.

4.2 | Bioactivity studies

In the present work, hCA I and II isoenzymes were purified by Sepharose-4B-L-tyrosine-sulfanilamide affinity column chromatography, CA isoenzymes' activity was determined according to the spectrophotometric method of Verpoorte et al.,[70] and *p*-nitrophenyl acetate (PNF) was used as a substrate for these isoenzymes.[71,72] For determination of inhibition kinetics of novel tetrafluoronaphthalene derivatives (**2**, **2a**, **4**–**6**), activity (%) and tetrafluoronaphthalene graphs were drawn. From these graphs, half maximal inhibitor concentrations (IC_{50}) for novel coumarin-1,2,3-triazole-acetamide hybrids were determined. Also, for K_i values, three different concentrations of novel tetrafluoronaphthalene derivatives (**2**, **2a**, **4**–**6**) were used. Then, Lineweaver–Burk[41] graphs were drawn according to these measurements. K_i values of novel tetrafluoronaphthalene derivatives (**2**, **2a**, **4**–**6**) were determined from Lineweaver–Burk graphs, as previously described.[73,74] The protein estimation was done by using Bradford's[75] method in which bovine serum albumin is used as a standard protein. The inhibitory effect of novel tetrafluoronaphthalene derivatives (**2**, **2a**, **4**–**6**) on AChE activity was determined according to the spectrophotometric method of Ellman et al.[76] In this study, 5,5′-dithio-bis(2-nitrobenzoic)acid (DTNB) was used for the estimation of the AChE enzyme activity. Briefly, 100 µl of buffer solution (pH 8.0, Tris/HCl, 1.0 M) and diverse concentration of sample solutions (30–300 µl) dissolved in deionized water were added to 50 µl of AChE enzyme solution (5.32×10^{-3} EU). Then, the mixtures were incubated for 10 min at 20°C. Finally, 50 µl of DTNB (0.5 mM and 25 ml) of substrate and acetylthiocholine iodide were added to incubated mixtures. Also, the reactions were initiated by the addition of 50 µl of acetylthiocholine iodide. The activity of AChE was evaluated spectrophotometrically at a wavelength of 412 nm.[77,78] The inhibitory effect of novel compounds on α-glycosidase enzyme activity was determined using *p*-nitrophenyl-D-glycopyranoside (*p*-NPG) substrate, according to the assay of Tao et al.[79] First, 200 µl of phosphate buffer was mixed with 40 µl of the homogenate solution in phosphate buffer (0.15 U/ml, pH 7.4). Also, 50 µl of *p*-NPG in phosphate buffer (5 mM, pH 7.4) after preincubation was added and again incubated at 30°C. The absorbances were spectrophotometrically measured at 405 nm according to previous studies.[80,81] The control activity was performed first for the IC_{50} study (only enzyme, buffer, substrate, and purified water were used), and then activity measurements were made at five different inhibitory concentrations. The last IC_{50} graph was drawn and then the IC_{50} value was calculated. In addition, we chose three of the five inhibitor concentrations we studied at IC_{50} for the K_i study, and then we created a table. Furthermore, activities at different substrate concentrations and different inhibitor concentrations were measured, and K_i graph was plotted (K_i values were calculated as inhibition was competitive or noncompetitive).

4.3 | Docking calculations

With theoretical calculations, preliminary information about the biological activities of molecules is gained. To obtain this information, calculations consisting of many stages should be made. First, the molecules are optimized using the Gaussian software program.[82] Files with *.sdf extension are created from the optimized structures obtained. Afterward, molecular docking calculations will be made using Maestro Molecular modeling platform (version 2020-4) by the Schrödinger program. In this program, the enzymatic proteins will be prepared first. The protein preparation module[83,84] was used for this. With this module, after the water molecules in the proteins were removed, the active sites of the enzyme proteins were determined. The protein molecules in this active area are given freedom of movement, thus facilitating their interaction. The LigPrep module[85,86] is then used to prepare the molecules for calculations. Then, calculations are made with the Glide ligand docking module[87] to interact with molecules and enzymes. Interactions will be examined with this module. ADME/T calculations are made to examine the use of molecules with high interactions as drugs. The Qik-prop module[88,89] of the Schrödinger software was used for ADME/T analysis. These calculations are used to predict how drug molecules will act and react in human metabolism.

ACKNOWLEDGMENTS

This study was made possible by TUBITAK ULAKBIM, High Performance and Grid Computing Center (TR-Grid e-Infrastructure). This study is supported by the Scientific Research Project ;Fund of Sivas Cumhuriyet University under project number RGD-020.

CONFLICTS OF INTERESTS

The authors declare that there are no conflicts of interests.

CREDIT AUTHORSHIP CONTRIBUTION STATEMENT

Musa Erdoğan: molecular design, synthesis, characterization, data analysis, writing-review, editing, supervision; Parham Taslimi: bioactivity studies, writing-review, editing; Burak Tuzun: molecular docking studies, writing-review, editing.

ORCID

Musa Erdoğan https://orcid.org/0000-0001-6097-2862
Parham Taslimi https://orcid.org/0000-0002-3171-0633
Burak Tuzun https://orcid.org/0000-0002-0420-2043

REFERENCES

[1] H. J. Böhm, D. Banner, S. Bendels, M. Kansy, B. Kuhn, K. Müller, M. Stahl, *ChemBioChem* **2004**, *5*(5), 637.
[2] E. P. Gillis, K. J. Eastman, M. D. Hill, D. J. Donnelly, N. A. Meanwell, *J. Med. Chem.* **2015**, *58*(21), 8315.
[3] K. Müller, C. Faeh, F. Diederich, *Science* **2007**, *317*(5846), 1881.
[4] M. Erdogan, S. Ozkinali, H. Mert, *J. Fluorine Chem.* **2021**, *242*, 109718.
[5] V. Církva, P. Jakubík, T. Strašák, J. Hrbáč, J. Sýkora, I. Císařová, J. Storch, *J. Org. Chem.* **2019**, 84(4), 1980.
[6] E. T. Akin, M. Erdogan, A. Dastan, N. Saracoglu, *Tetrahedron* **2017**, *73*(37), 5537.
[7] J. Wang, B. Huang, Y. Gao, C. Yang, W. Xia, *J. Org. Chem.* **2019**, *84*(11), 6895.
[8] P. J. Xia, Z. P. Ye, Y. Z. Hu, J. A. Xiao, K. Chen, H. Y. Xiang, H. Yang, *Org. Lett.* **2020**, *22*(5), 1742.
[9] K. Funabiki, Y. Saito, T. Kikuchi, K. Yagi, Y. Kubota, T. Inuzuka, S. Kutsumizu, *J. Org. Chem.* **2019**, *84*(7), 4372.
[10] K. C. Rippy, N. J. DeWeerd, I. V. Kuvychko, Y. S. Chen, S. H. Strauss, O. V. Boltalina, *ChemPlusChem* **2018**, *83*(12), 1067.
[11] K. Takahashi, M. Shimoi, T. Watanabe, K. Maeda, S. J. Geib, D. P. Curran, T. Taniguchi, *Org. Lett.* **2020**, *22*(5), 2054.
[12] C. Isanbor, D. O'Hagan, *J. Fluorine Chem.* **2006**, *127*(3), 303.
[13] H. Amii, K. Uneyama, *Chem. Rev.* **2009**, *109*(5), 2119.
[14] B. Ngameni, K. Cedric, A. T. Mbaveng, M. Erdogan, I. Simo, V. Kuete, A. Dastan, *Bioorg. Med. Chem. Lett.* **2021**, *35*, 127827.
[15] R. H. Hans, E. M. Guantai, C. Lategan, P. J. Smith, B. Wan, S. G. Franzblau, K. Chibale, *Bioorg. Med. Chem. Lett.* **2010**, *20*, 942.
[16] J. C. Espinoza-Hicks, K. F. Chacón-Vargas, J. L. Hernández-Rivera, B. Nogueda-Torres, J. Tamariz, L. E. Sánchez-Torres, A. Camacho-Dávila, *Eur. J. Med. Chem.* **2019**, *167*, 402.
[17] P. Devendar, A. N. Kumar, M. S. Bethu, A. Zehra, R. Pamanji, J. V. Rao, J. K. Kumar, *RSC Adv.* **2015**, *5*(113), 93122.
[18] F. Erdemir, D. Barut Celepci, A. Aktas, Y. Gok, R. Kaya, P. Taslimi, Y. Demir, I. Gülcin, *Bioorg. Chem.* **2019**, *91*, 103134.
[19] M. Boztas, P. Taslimi, M. A. Yavari, İ. Gülçin, E. Sahin, A. Menzek, *Bioorg. Chem.* **2019**, *89*, 103017.
[20] F. Türkan, A. Cetin, P. Taslimi, H. S. Karaman, I. Gulcin, *Arch. Pharm.* **2019**, *352*(6), e1800359.
[21] A. Maharramov, R. Kaya, P. Taslimi, M. Kurbanova, A. Sadigova, V. Farzaliyev, A. Sujayev, I. Gulcin, *Arch. Pharm.* **2019**, *352*(2), e1800317.
[22] E. Güzel, U. M. Kocyigit, B. S. Arslan, M. Atas, P. Taslimi, F. Gokalp, M. Nebioglu, I. Sisman, I. Gulcin, *Arch. Pharm.* **2019**, *352*(2), e1800292.
[23] P. Taslimi, *Arch. Pharm.* **2020**, *353*, e2000210. https://doi.org/10.1002/ardp.202000210
[24] I. Gulcin, P. Taslimi, A. Aygün, N. Sadeghian, E. Bastem, O. I. Kufrevioglu, F. Turkan, F. Sen, *Int. J. Biol. Macromol.* **2018**, *119*, 741.
[25] F. Türker, D. Barut Celepci, A. Aktas, P. Taslimi, Y. Gök, M. Aygün, I. Gulcin, *Arch. Pharm.* **2018**, *351*(7), e201800029.
[26] P. Taslimi, C. Caglayan, F. Farzaliyev, O. Nabiyev, A. Sujayev, F. Türkan, R. Kaya, I. Gulcin, *J. Biochem. Mol. Toxicol.* **2018**, *32*(4), e22042.
[27] Y. Demir, P. Taslimi, M. S. Özaslan, N. Oztaskin, Y. Cetinkaya, I. Gulcin, S. Beydemir, S. Goksu, *Arch. Pharm.* **2018**, *351*, 1800263.
[28] B. Tuzun, *Turk. Comput. Theor. Chem.* **2020**, *4*(2), 76.
[29] A. Aktas, B. Tüzün, R. Aslan, K. Sayin, H. Ataseven, *J. Biomol. Struct. Dyn.* **2020**, 111
[30] M. A. Gedikli, B. Tuzun, A. Aktas, K. Sayin, H. Ataseven, *Bratisl. Lek. Listy* **2021**, *122*(2), 101.
[31] V. Alterio, S. M. Monti, E. Truppo, C. Pedone, C. T. Supuran, G. De Simone, *Org. Biomol. Chem.* **2010**, *8*, 3528.
[32] J. Ivanova, J. Leitans, M. Tanc, A. Kazaks, R. Zalubovskis, C. T. Supuran, K. Tars, *Chem. Commun. (Camb).* **2015**, *51*(33), 7108.
[33] J. Cheung, E. N. Gary, K. Shiomi, T. L. Rosenberry, *ACS Med. Chem. Lett.* **2013**, *4*, 1091.
[34] S. C. Garman, D. N. Garboczi, *J. Mol. Biol.* **2004**, *337*(2), 319.
[35] G. W. Gribble, C. S. LeHoullier, M. P. Sibi, R. W. Allen, *J. Org. Chem.* **1985**, *50*(10), 1611.
[36] S. Burmaoglu, A. O. Yilmaz, P. Taslimi, O. Algul, D. Kılıc, I. Gulcin, *Arch. Pharm.* **2018**, *351*(2), e1700314.
[37] F. Erdemir, D. Barut Celepci, A. Aktas, P. Taslimi, Y. Gök, H. Karabıyık, I. Gulcin, *J. Mol. Struct.* **2018**, *1155*, 797.
[38] U. M. Kocyigit, Y. Budak, F. Eliguzel, P. Taslimi, D. Kılıc, I. Gulcin, M. Ceylan, *Arch. Pharm.* **2017**, *350*(12), e1700198.
[39] A. Aktas, P. Taslimi, I. Gulcin, Y. Gök, *Arch. Pharm.* **2017**, *350*(6), e1700045.
[40] C. Bayrak, P. Taslimi, I. Gulcin, A. Menzek, *Bioorg. Chem.* **2017**, *72*, 359.
[41] H. Lineweaver, D. Burk, *J. Am. Chem. Soc.* **1934**, *56*, 658.
[42] P. Taslimi, A. Sujayev, S. Mamedova, P. Kalın, I. Gulcin, N. Sadeghian, S. Beydemir, O. I. Küfrevioglu, S. H. Alwasel, V. Farzaliyev, S. Mamedov, *J. Enzyme Inhib. Med. Chem.* **2017**, *32*(1), 137.
[43] K. Aksu, B. Ozgeris, P. Taslimi, A. Naderi, I. Gulcin, S. Göksu, *Arch. Pharm.* **2016**, *349*(12), 944.
[44] P. Taslimi, I. Gulcin, B. Ozgeris, S. Goksu, F. Tumer, S. H. Alwasel, C. T. Supuran, *J. Enzyme Inhib. Med. Chem.* **2016**, *31*(1), 152.
[45] H. I. Gül, K. Kucukoglu, C. Yamali, S. Bilginer, H. Yuca, I. Ozturk, P. Taslimi, I. Gulcin, C. T. Supuran, *J. Enzyme Inhib. Med. Chem.* **2016**, *31*(4), 568.
[46] C. Yamali, H. I. Gül, A. Ece, P. Taslimi, I. Gulcin, *Chem. Biol. Drug Des.* **2018**, *91*(4), 854.
[47] M. Rezai, C. Bayrak, P. Taslimi, I. Gulcin, A. Menzek, *Turk. J. Chem.* **2018**, *42*(3), 808.
[48] P. Taslimi, I. Gulcin, *J. Food Biochem.* **2018**, *42*(3), e12516.
[49] I. Gulcin, P. Taslimi, *Expert Opin. Ther. Pat.* **2018**, *28*(7), 541.
[50] B. Yigit, M. Yigit, D. Barut Celepci, Y. Gök, A. Aktas, M. Aygün, P. Taslimi, I. Gulcin, *ChemistrySelect* **2018**, *3*(27), 7976.
[51] M. Zengin, H. Genc, P. Taslimi, A. Kestane, E. Guclu, A. Ogutlu, O. Karabay, I. Gulcin, *Bioorg. Chem.* **2018**, *81*, 119.
[52] A. Aktas, B. Tuzun, A. H. Taskin, K. Sayin, H. Ataseven, *Bratisl. Lek. Listy* **2020**, *121*(10), 705.
[53] E. Cetiner, K. Sayın, B. Tuzun, H. Ataseven, *Bratisl. Lek. Listy* **2021**, 122. https://doi.org/10.4149/BLL_2021_44
[54] K. Sayin, A. Ungordu, *Spectrochim. Acta, Part A* **2019**, *220*, 117102.
[55] K. Sayin, D. Karakas, *Spectrochim. Acta, Part A* **2018**, *202*, 276.
[56] K. Sayin, D. Karakas, *J. Mol. Struct.* **2018**, *1158*, 57.
[57] K. Sayin, A. Ungordu, *Spectrochim. Acta, Part A* **2018**, *193*, 147.
[58] K. Sayin, D. Karakas, *J. Mol. Struct.* **2017**, *1146*, 191.

[59] S. Boy, F. Türkan, M. Beytur, A. Aras, O. Akyildirim, H.S. Karaman, H. Yüksek, *Bioorg. Chem.* **2021**, *107*, 104524.
[60] A. Ungordu, K. Sayin, *Chem. Phys. Lett.* **2019**, *733*, 136677.
[61] H. Gezegen, M. B. Gürdere, A. Dincer, O. Ozbek, U. M. Kocyigit, P. Taslimi, M. Ceylan, *Arch. Pharm.* **2020**, e2000334. https://doi.org/10.1002/ardp.202000334
[62] U. M. Kocyigit, P. Taslimi, B. Tuzun, H. Yakan, H. Muglu, E. Güzel, *J. Biomol. Struct. Dyn.* **2020**, 111
[63] P. Taslimi, F. Turkan, D. Gungordu Solgun, A. Aras, Y. Erden, H. U. Celebioglu, I. Gulcin, *J. Biomol. Struct. Dyn.* **2020**, 112
[64] P. Taslimi, U. M. Kocyigit, B. Tuzun, M. Kirici, *J. Biomol. Struct. Dyn.* **2020**, 19
[65] A. Huseynova, R. Kaya, P. Taslimi, V. Farzaliyev, X. Mammadyarova, A. Sujayev, I. Gulcin, *J. Biomol. Struct. Dyn.* **2020**, 113
[66] C. A. Lipinski, *Drug Discovery Today: Technol.* **2004**, *1*, 337.
[67] C. A. Lipinski, F. Lombardo, B. W. P. J. Dominy Feeney, *Adv. Drug Delivery Rev.* **1997**, *23*, 3.
[68] W. J., Jorgensen, E. M., Duffy, *Adv. Drug Delivery Rev.* **2002**, *54*, 355.
[69] M. Huseynova, P. Taslimi, A. Medjidov, V. Farzaliyev, M. Aliyeva, G. Gondolova, O. Sahin, B. Yalcın, A. Sujayev, E. B. Orman, A. R. Ozkaya, I. Gulcin, *Polyhedron* **2018**, *155*, 25.
[70] J. A. Verpoorte, S. Mehta, T. J. Edsall, *J. Biol. Chem.* **1967**, *242*, 4221.
[71] B. Yigit, R. Kaya, P. Taslimi, Y. Isık, M. Karaman, M. Yigit, I. Özdemir, I. Gulcin, *J. Mol. Struct.* **2019**, *1179*, 709.
[72] I. Timur, U. M. Kocyigit, T. Dastan, S. Sandal, A. O. Ceribasi, P. Taslimi, I. Gulcin, M. Koparir, M. Karatepe, M. Ciftci, *J. Biochem. Mol. Toxicol.* **2019**, *33*(*1*), e22239.
[73] N. Eruygur, M. Atas, M. Tekin, P. Taslimi, U. M. Kocyigit, I. Gulcin, *S. Afr. J. Bot.* **2019**, *120*, 141.
[74] B. Kuzu, M. Tan, P. Taslimi, I. Gulcin, M. Taspınar, N. Menges, *Bioorg. Chem.* **2019**, *86*, 187.
[75] M. M. Bradford, *Anal. Biochem.* **1976**, *72*, 248.
[76] G. L. Ellman, K. D. Courtney, V. Andres, R. M. Featherston, *Biochem. Pharmacol.* **1961**, *7*, 88.
[77] C. Caglayan, Y. Demir, S. Kücükler, P. Taslimi, F. M. Kandemir, I. Gulcin, *J. Food Biochem.* **2019**, *43*(*2*), e12720.
[78] E. Bursal, A. Aras, O. Kılıc, P. Taslimi, A. C. Gören, I. Gulcin, *J. Food Biochem.* **2019**, *43*(*3*), e12776.
[79] Y. Tao, Y. Zhang, Y. Cheng, Y. Wang, *Biomed. Chrom.* **2013**, *27*, 148.
[80] R. Kaya, P. Taslimi, M. E. Naldan, I. Gulcin, *Lett. Drug Des. Discovery* **2019**, *14*(*5*), 573.
[81] H. Genc Bilgicli, A. Kestane, P. Taslimi, O. Karabay, A. Bytyqi-Damoni, M. Zengin, I. Gulcin, *Bioorg. Chem.* **2019**, *88*, 102931.
[82] M. J. Frisch, G. W. Trucks, H. B. Schlegel, G. E. Scuseria, M. A. Robb, J. R. Cheeseman, G. Scalmani, V. Barone, G. A. Petersson, H. Nakatsuji, X. Li, M. Caricato, A. Marenich, J. Bloino, B. G. Janesko, R. Gomperts, B. Mennucci, H. P. Hratchian, J. V. Ortiz, A. F. Izmaylov, J. L. Sonnenberg, D. Williams-Young, F. Ding, F. Lipparini, F. Egidi, J. Goings, B. Peng, A. Petrone, T. Henderson, D. Ranasinghe, V. G. Zakrzewski, J. Gao, N. Rega, G. Zheng, W. Liang, M. Hada, M. Ehara, K. Toyota, R. Fukuda, J. Hasegawa, M. Ishida, T. Nakajima, Y. Honda, O. Kitao, H. Nakai, T. Vreven, K. Throssell, J. A. Montgomery, Jr., J. E. Peralta, F. Ogliaro, M. Bearpark, J. J. Heyd, E. Brothers, K. N. Kudin, V. N. Staroverov, T. Keith, R. Kobayashi, J. Normand, K. Raghavachari, A. Rendell, J. C. Burant, S. S. Iyengar, J. Tomasi, M. Cossi, J. M. Millam, M. Klene, C. Adamo, R. Cammi, J. W. Ochterski, R. L. Martin, K. Morokuma, O. Farkas, J. B. Foresman, J. V. Ortiz, J. Cioslowski, D. J. Fox, *Gaussian 09*, *Revision D.01*, Gaussian Inc., Wallingford, CT **2009**.
[83] L. Schrodinger, Small-Molecule Drug Discovery Suite–42019, **2019**.
[84] Schrödinger Release 2019-4: Protein Preparation Wizard; Epik, Schrödinger, LLC, New York, NY **2016**; Impact, Schrödinger, LLC, New York, NY **2016**; Prime, Schrödinger, LLC, New York, NY **2019**.
[85] R. A. Friesner, R. B. Murphy, M. P. Repasky, L. L. Frye, J. R. Greenwood, T. A. Halgren, P. C. Sanschagrin, D. T. Mainz, *J. Med. Chem.* **2006**, *49*, 6177.
[86] G. M. Sastry, M. Adzhigirey, T. Day, R. Annabhimoju, W. Sherman, *J. Comput.-Aided Mol. Des.* **2013**, *27*, 221.
[87] Schrödinger Release 2019-4: LigPrep, Schrödinger, LLC, New York, NY **2019**.
[88] Q. Du, Y. Qian, X. Yao, W. Xue, *J. Biomol. Struct. Dyn.* **2020**, *38*, 625.
[89] R. Schrödinger 2: QikProp. Schrödinger, LLC, New York, NY, 2018.

SUPPORTING INFORMATION

Additional Supporting Information may be found online in the supporting information tab for this article.

How to cite this article: M. Erdoğan, P. Taslimi, B. Tuzun. Synthesis and docking calculations of tetrafluoronaphthalene derivatives and their inhibition profiles against some metabolic enzymes. *Arch. Pharm.* **2021**, 354, e2000409. https://doi.org/10.1002/ardp.202000409